UDC 541.6:547.6

DFT INVESTIGATION ON THE DOUBLE HYDROGEN-BONDED SYSTEM: THE OXIDATION AND HYDRATION EFFECT

P.Y. Cui, B.P. Liu, S. Yan

School of Chemistry and Chemical Engineering, Qufu Normal University, Qufu, China,
e-mail: pinglysh@gmail.com

The trustworthy B3LYP/6-311+G* method is employed to investigate the double hydrogen-bonded system with a special emphasis on the oxidation and hydration effect. Proton transfer occurs spontaneously upon oxidation from the amido group to the adjacent imidazole fragment. The larger the pH value of the environment, the significant the effect on the geometry structure is. The electron population on the HOMO determines the IR vibrational frequency of the H bond, being blue-shift or red-shift. The complex prefers to be oxidized under the basic condition. The weak acidic environment is recommended to prevent the DNA mutation.

K e y w o r d s: density functional theory, oxidation effect, frontier molecular orbital, ionization potential, double hydrogen-bonded system.

INTRODUCTION

DNA damage and the corresponding structural variations of the base pairs have attracted many experimental and theoretical efforts. Generally, the DNA damage may originate from radiations, chemical reactions, and electron attachment/detachment. These ways are interrelated and coupled with each other, which makes the damage mechanism more complicated. Single electron reduction/oxidation, caused by electron attachment/detachment, is ubiquitous in physical, chemical, and biological systems. The appropriate redox reaction provides the driving force for the chemical process, photosynthesis and respiration, and operation of living things, while the improper process causes the DNA mutation, resulting in various diseases such as cancer. When electron transfer is coupled with the proton shift, the mechanism becomes more enigmatic. The coupling of proton chemistry with redox reactions is important in many enzymes and is central to energy transfer in biology.

DNA triplexes have received considerable attention because of their potential for both the control of gene expression and as therapeutic agents [1—4]. Although the triplex is affected by numerous contributions, such as stacking, hydration, counterions, phosphate environment, backbone restrictions, the H bond is the predominant interaction that determines the structure and dynamics of DNA triplexes. A recent special work carried out with the density functional theory method was focused on the H bonds of DNA triplexes [5]. The imidazole ring (ImH) is an essential constituent of many biological compounds, such as adenine, guanine, histamine, and the histidine residues of proteins. The unique ring structure of ImH permits it as the H-bridge because one proton can be picked up by the bare N atom and the other one can be released from another N atom. This action has been employed to explain the proton conductivity properties [6, 7] of solid ImH material and also in the actual biological surrounding where a long H-bonded chain is present; many investigations have been carried out in both experimental [8—11] and theoretical [12—15] fields.

Adenine, an elementary chemical component of DNA, RNA, and adenosine triphosphate (ATP), playing an essential role in replication in all known living systems, is significant in many other aspects

of biochemistry, including cellular respiration and protein synthesis [16—19]. The dehydrogenation of adenine and the H atom loss in pyrimidine DNA bases induced by low-energy electrons have been explored [20, 21]. The relatively high activity of the adenine N_9 site has been suggested in the previous experimental and theoretical studies [22—24]. Dehydrogenated adenine (**DA**) has been observed in these investigations, while no related discussions can be found yet. Recently, the noncovalent interaction between adenine and ImH has been reported [25]. The investigation on the triplex ImH-adenine-ImH (**HIAIH**) that has been taken as the prototype model in our previous work [26] should furnish some significant and detailed information about the structure and the properties of biomolecular systems.

As is known, the coupling of base pairs is achieved through multi-hydrogen bonds, therefore, only the matrices involving double H bonds between **DA** and ImHs are considered here. In the present work, the coupling characteristic, the corresponding IR frequency shifts, the frontier molecular orbitals, and charge populations as well as the energy changes are investigated based on the double hydrogen-bonded ImH-dehydrogenated adenine-ImH trimer (**HIDAIH**).

COMPUTATIONAL DETAILS

Hybrid density functional (DFT) methods have proven to be successful in describing nucleic base dimers [27] and DNA triplex [5]. Especially, the B3LYP hybrid functional is found to be reliable for geometry optimizations and property explorations [28, 29]. Therefore, all calculations, including the geometry optimization, IR frequency, and the related energies were performed employing the B3LYP functional equipped with a 6-311+G(d) basis set, implemented with the Gaussian 03 program [30]. To clarify whether the optimized structures correspond to the genuine local minima on the global potential energy surface or not, the vibrational frequency analyses were carried out at the same level. The related energy calculations were all corrected with the zero-point energy that was obtained in the IR frequency calculation. The oxidation occurs when the electron is detached from the highest occupied molecular orbital (HOMO), and the corresponding energy change is defined as the ionization potential (IP). Any bond length variations should reflect the electron density pattern of the HOMO. Those in bonding regions should be weakened and lengthened, while those located in anti-bonding regions should be strengthened and therefore shortened. For the selected model (**HIDAIH**) the odd electron occupies the HOMO, therefore, the lowest unoccupied molecular orbital (LUMO) of the oxidized system corresponds to the HOMO of **HIDAIH**. Thus, the HOMO and LUMO are all explored for the inspection of the oxidation and hydration effect. The spin density analyses were also performed to investigate the charge population on oxidation and hydration.

The basicity varies upon both proton dissociation and hydration with the H bond formation, which can be reflected experimentally by the pH value in the solution. Thus, in order to provide some useful information to the experimentalist, deprotonated ImH and hydrated ImH are all explored to investigate the influence of basic variation.

RESULTS AND DISCUSSION

The atomic numbering of dehydrogenated adenine (**DA**) is shown in Fig. 1. The optimized geometry parameters of **DA**, reduced **DA**, and oxidized **DA** are collected in Table 1. The primary bond lengths of the optimized model system (**HIDAIH**), deprotonated imidazole-dehydrogenated adenine-imidazole (**IDAIH⁻**) triplex, hydrated **HIDAIH** (**HIDAIHW**), and hydroxyl-**HIDAIH** (**HIDAIHOH⁻**) as well as the corresponding oxidized complexes are all represented in Fig. 2. IR frequencies of these trimers are described in Fig. 3 and the assignment of the H bonds with distinct IR intensity is performed. The charge populations of the optimized complexes are delineated in Fig. 4. Fig. 5 represents the HOMO, LUMO, and spin densities of these trimers.

According to our experience on **HIAIH** [26], it is significant to explore the electronic effect on **DA**. Table 1 demonstrates that the bond length variations upon electron attachment are inverse to those on oxidation. This phenomenon is different from our findings on adenine as declares that the effect introduced by adenine hydrogen loss is distinguished. Similar to that of adenine, C_6—N_6 re-
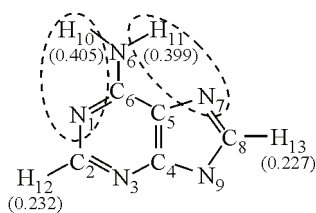
Fig. 1 (*left*). Atomic numbering of de-hydrogenated adenine (**DA**). The charges on **DA** hydrogen are shown in parentheses
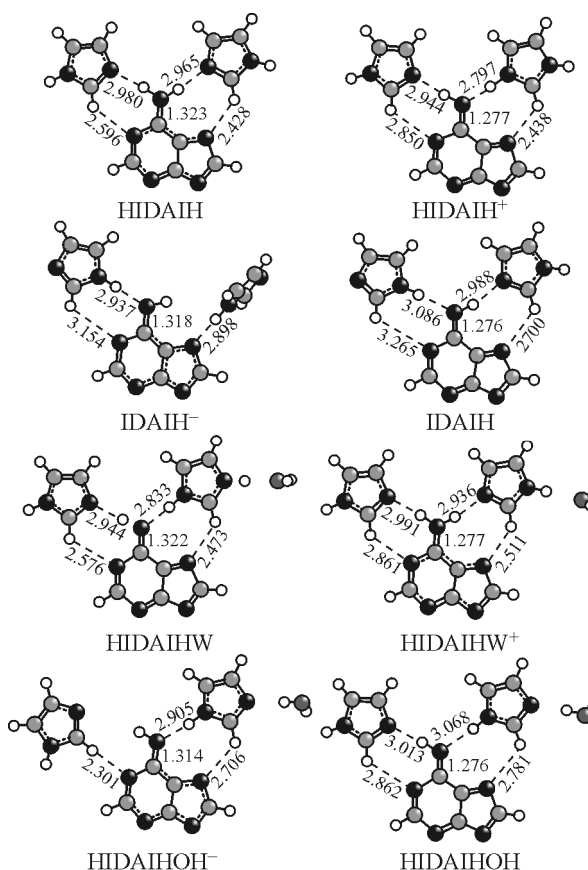

Fig. 2 (*right*). Primary H-bond parameters of the investigated complexes

duces upon oxidation, while it lengthens upon electron capture. The positive charge population of **DA** shown in Fig. 1 illustrates that N_6—Hs prefer to participate in the H bond formation with ImH fragments. The oxidation of **DA** is endothermic (194.6 kcal/mol), which stands between adenine (186.8 kcal/mol) and ImH (201.1 kcal/mol), while its reduction is an exothermic process (–74.3 kcal/mol), which is inverse to adenine (8.6 kcal/mol) and ImH (19.7 kcal/mol). As is indicated, **DA** prefers to capture an electron and is not easily oxidized, while an oxidative damage to DNA plays a key role in mutagenesis and carcinogenesis, which has recently attracted considerable interest [31—33]. Therefore, only the oxidation effect on the trimer is investigated in the following.

Geometric characteristics. The primary H bond parameters and the optimized triplex structures are all represented in Fig. 2. As shown in the figure, two H bonds (N…H—C and N_6—H…N) are generated between adenine and each ImH fragment of **HIDAIH**. Although the H atom has been detached

Table 1

Primary bond lengths (Å) *of dehydrogenated adenine* (**DA**), *reduced* **DA**, *and oxidized* **DA** *obtained at the* B3LYP/6-311+G* *level*

Bond	Reduced **DA**	**DA**	Oxidized **DA**	Bond	Reduced **DA**	**DA**	Oxidized **DA**
N_1C_2	1.354	1.330	1.305	C_5N_7	1.374	1.322	1.276
N_1C_6	1.341	1.347	1.362	C_6N_6	1.375	1.339	1.301
C_2N_3	1.323	1.361	1.414	N_6H	1.004	1.009	1.017
C_2H	1.090	1.086	1.086	N_7C_8	1.346	1.413	1.495
N_3C_4	1.360	1.314	1.278	C_8N_9	1.354	1.309	1.279
C_4C_5	1.420	1.448	1.488	C_8H	1.087	1.083	1.082
C_4N_9	1.361	1.387	1.405				

from the N_9 site of adenine, the influence on these four H bonds is very weak and no change is found as compared to **HIAIH** [38]. Thus, it is presumed that the variation of H dissociation from N_9 on charge population of adenine is feeble. Upon oxidation, the proton transfers spontaneously from N_6 to bare N of right ImH. Such a phenomenon has been observed in **HIAIH** and ImH dimer [19] systems. The reduction of two central N—H…N bonds and the lengthening of two peripheral C—H…N bonds upon oxidation are also illustrated by Fig. 2; it suggests that the electron density on the adenine framework decreases upon oxidation. The double bond characteristic of C_6N_6 increases, which is represented by the reduced bond length.

The pH value enhances when the proton is detached from bonded N of left ImH, **IDAIH⁻**. The influence of this proton detachment on the geometry structure is significant, as displayed in Fig. 2. First of all, the proton is pulled by the left ImH fragment from N_6 due to its strong basicity. This proton transfer results in the basic enhancement of adenine coupled with the decrease in the proton donor capability and the increase in the proton acceptor ability. Second, right ImH rolls and rotates, resulting in the breaking of original double H bonds and the formation of a novel N_7…H—N bond with the right ImH fragment that is perpendicular to adenine. For the oxidized triplex **HIDAIH⁺**, when the proton is peeled off from the left ImH fragment of **IDAIH**, the transferred proton locates back to N_6 and another proton on N_6 can be transferred spontaneously to the left ImH fragment where the proton detachment occurs, followed by the lengthening of all H bonds. During this process, there is no distinct variation of the C_6N_6 bond that still carries typical double bond characteristics.

The basicity of right ImH increases when a water molecule binds to it through the H bond. Accordingly, as compared with **HIDAIH**, the N_6—H…N bond length between adenine and right ImH of **HIDAIHW** reduces, while the C—H…N bond increases owing to the strengthening of the C—H coupling. It can also be concluded that basicity variation owing to water binding is less significant as compared to that upon proton detachment. Similar to **HIDAIH**, the proton transfers spontaneously to right ImH as an electron is eliminated from **HIDAIHW**.

For the hydroxyl bonded ImH, the pH value is stronger than that of hydrated ImH, while it is weaker as compared to that of deprotonated ImH. Therefore, the geometry variations of the **HIDAI-HOH⁻** triplex should be larger as compared to the alterations of **HIDAIHW** and less than the changes in **IDAIH⁻**. As is illustrated distinctly in Fig. 2, the proton on N_6 transfers spontaneously to the right ImH fragment whose basicity is enhanced. The N_6—H…N bond between adenine and another ImH is broken with the rolling of ImH around the C—H…N bond. Although left ImH is still in the same plane with adenine, there is only the C—H…N bond and the electrostatic interaction between electronegative N(ImH) and electropositive H(N_6). Another spontaneous proton transfer is observed between ImH and the hydroxyl group, which demonstrates that OH is a strong base. Upon oxidation, the double bond characteristic of C_6N_6 increases and N_6—H…N is regenerated with left ImH rolling back.

By extrapolation, proton transfer occurs spontaneously under a strong basic environment or upon oxidation. If the base is sufficiently strong, the rolling, or even the rotation of another ImH fragment occurs easily.

IR frequencies. IR spectroscopy is one of the standard methods to investigate molecular structures, providing the information about the structural details, including H bonds and the protonation status of chemical groups at the active site. The IR vibrational frequency analyses are performed to get related structural information as well as to validate the triplexes corresponding to the local minima on the global potential energy surface.

Fig. 3 collects the harmonic vibrational IR spectra of all optimized triplexes. The IR spectra of the H bonds involving the N_6H group carry significant intensity, and they are assigned in the figure. Two N_6H…N stretching vibrational modes of **HIDAIH** combined together generate the symmetric N—H…N and anti-symmetric N—H…N stretching modes at 3207.8 cm⁻¹ and 3314.6 cm⁻¹ respectively. After oxidation, these two stretching modes are red-shifted in different degree. The N_6—H…N stretching is assigned at 3036.9 cm⁻¹, while the vibration at 2766.7 cm⁻¹ is assigned as the N_6…H—N mode, which is red-shifted by more than 500 cm⁻¹ owing to its electron density reduction. The spectra variation of the N_6…H—N stretching mode is small although the proton transfers upon proton detachment on left ImH, as illustrated by the similar electron environment before and after proton disso-
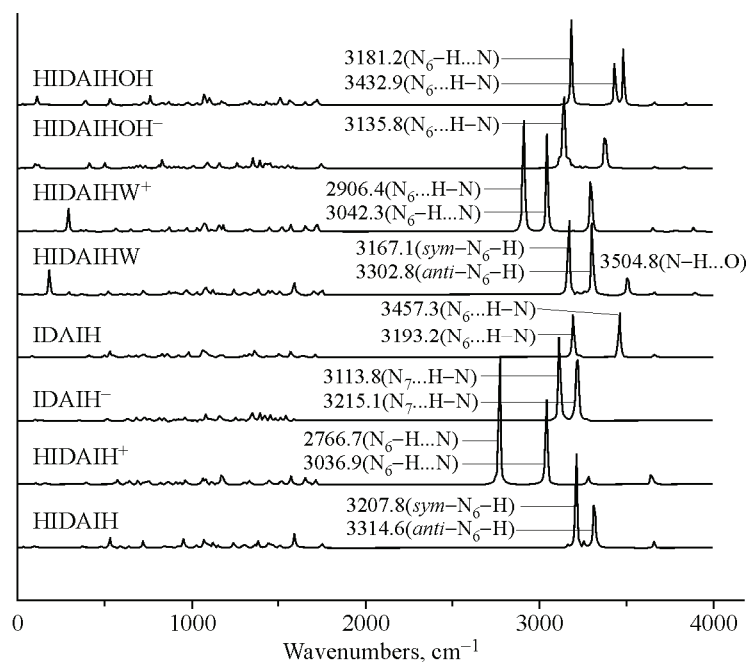
Fig. 3. IR spectra of the complexes obtained at the B3LYP/6-311+G* level

ciation. Another N_6—H…N stretching disappears for the rotation of the right ImH fragment, and another mode with strong intensity at 3113.8 cm^{-1} is assigned to N_7…H—N stretching. For the oxidized **IDAIH** system, the assignments are performed for N_6…H—N and N_6—H…N stretching modes at 3457.3 cm^{-1} and 3193.2 cm^{-1} respectively. As compared with the IR spectra of **IDAIH$^-$**, a distinct blue shift can be observed for N_6…H—N stretching when the system is oxidized. The blue shift of the H bond upon oxidation has attracted extensive attention [15, 34, 35]. The vibrational stretching of two N_6—H…N modes is slightly red-shifted (3167.1 cm^{-1} and 3302.8 cm^{-1}) upon hydration owing to the weakening of two H bonds due to the basic enhancement of right ImH. These two modes are distinctly red-shifted in the oxidized **HIDAIHW$^+$** system; although it is not as significant as that in **HIDAIH**, the phenomenon is similar. Only one N_6…H—N bond stretching with strong intensity can be found at 3135.8 cm^{-1} in the hydroxyl bonded system **HIDAIHOH$^-$**. Another one with strong intensity corresponds to the N…H—O stretching, which can be found in both hydrated and hydroxyl bonded systems. After the electron detachment, N_6…H—N stretching is blue-shifted by 300 cm^{-1}, which originates from the electron density decreasing on the **DA** fragment. Another N_6—H…N stretching is assigned at 3181.2 cm^{-1}.

It can be observed that IR spectroscopy may support some complementary information for the geometric structure, especially for the H bond. Furthermore, the calculated IR information can be compared with the experimental data to verify the reliability of the selected theoretical method. Thus, IR spectroscopy is a very useful tool for both experimentalists and theoreticians.

Charge populations. The nature of the variation reflected by the geometry structure and the IR frequency can be traced from charge populations. Fig. 4 represents the charge populations on each fragment of the optimized complexes. With the analyses on the charge popula- tions, we can obtain...
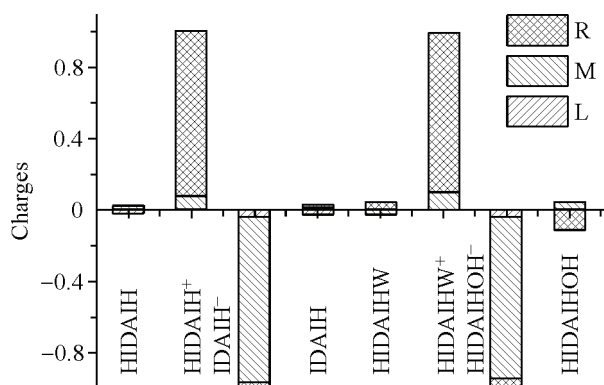

Fig. 4. Charge populations of the optimized complexes. R refers to the right imidazole fragment, M is dehydrogenated adenine, and L denotes the left imidazole fragment
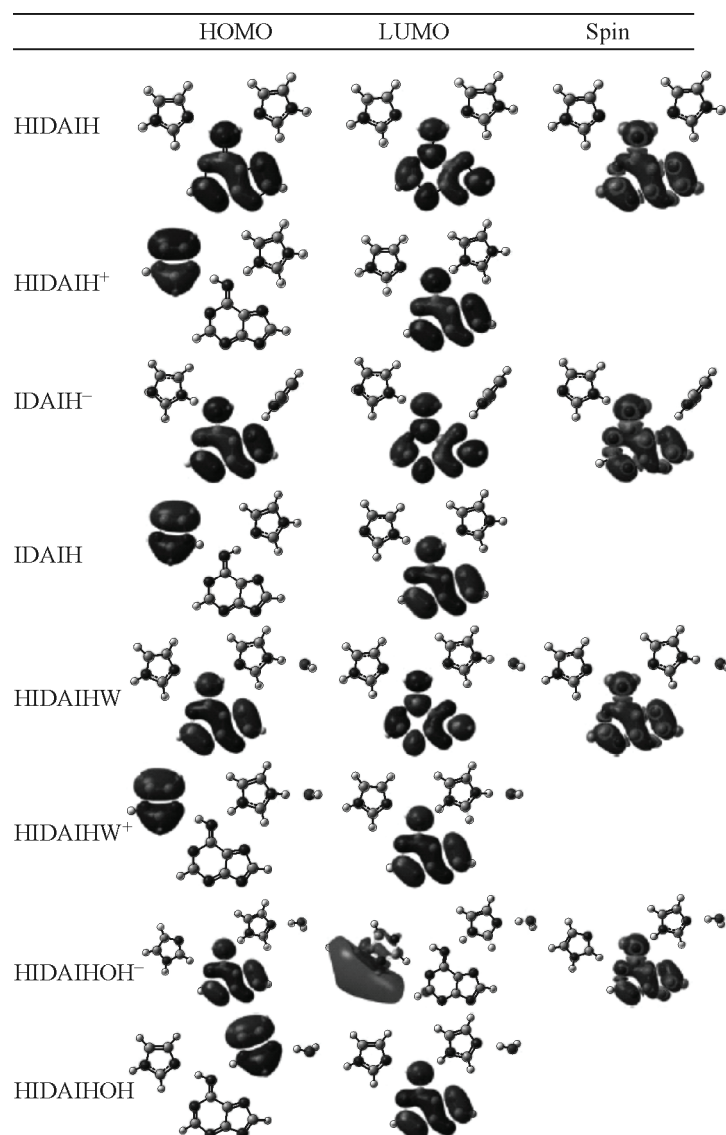
Fig. 5. HOMO, LUMO, and spin density of the optimized complexes

tion and the bonding mode, it is supposed to furnish some underlying information to explain the geo-metric structure changes and IR frequency alterations. Upon oxidation, electron detachment occurs usually on the HOMO, from which some significant information about the geometry variation and the IR spectral shift upon oxidation can be obtained. After oxidation, the HOMO corresponds to the LUMO of the oxidized system when there is only one electron on this HOMO. It is effective espe-cially in the analysis on the H bond variation [15]. The HOMO, LUMO, and spin densities of the in-vestigated complexes are collected in Fig. 5.

There is no charge on each fragment of the neutral triplex system **HIDAIH**, as shown in Fig. 4. The single electron occupies the HOMO and locates on **DA** (Fig. 5). The N_6H group is involved in the HOMO region. Upon oxidation by electron detachment, the system carries one positive charge, almost all of which locates on the right ImH fragment (Fig. 4). Thus, it is the proton rather than hydrogen that is transferred from N_6 to right ImH. The HOMO locates on left ImH now and the N_6H coupling is weakened. Therefore, the red shifts of two H bonds are observed in the IR spectrum. When a proton is detached from left ImH of **HIDAIH**, the negative charge should remain on left ImH, while Fig. 4 tells us that almost all negative charge locates on the middle **DA** fragment. Therefore, it is the proton rather than the H atom that is transferred from N_6 to left ImH and a single electron is still left on **DA**. The

HOMO located on **DA** attracts ImH H(N) and reduces the NH coupling, leading to the red shifts of two H bonds. The oxidation of **IDAIH**$^-$ generates a neutral system and there is no charge on each fragment (Fig. 4). The HOMO located on left ImH attracts H in N—H…N$_6$, leading to the strengthening of the NH coupling and a blue shift of this H bond. Three fragments of the hydrated **HIDAIHW** triplex possess near-zero charges, similar to those of **HIDAIH**. The frontier orbitals are similar to those of **HIDAIH**. After oxidation, one positive charge is left on the right ImH fragment of the system and no odd electron remains. Here, it still should be proton transfer from N$_6$ to right ImH. The hydroxyl bonded system **HIDAIHOH**$^-$ bears one negative charge on the **DA** fragment. Therefore, we can definitely say that they are consecutive proton transfers from N$_6$ to the hydroxyl group through right ImH. For the oxidized system, no significant charge can be found on each fragment. The detached electron should be the odd one located on **DA**. The HOMO of **HIDAIHOH** located on the right ImH fragment attracts H in the N$_6$…H—N bond, leading to the strengthening of the NH coupling and a blue shift of this H bond.

The spin density demonstrates the single electron population. Here, the spin density populations of all complexes with a single electron indicate that the single electron locates on the **DA** fragment, supporting the results obtained from HOMO analyses.

Ionization potential. The adiabatic ionization potentials (IPs) are determined at the B3LYP/6-311+G(d) level. It has been reported that the IP of **HIAIH** is 161.5 kcal/mol [38]. For the dehydrogenated **HIDAIH** system the IP is 163.3 kcal/mol, which is almost equal to that of **HIAIH**. Therefore, the effect of hydrogen detachment from the N$_9$ site on the IP is weak. If the proton on N of the left ImH fragment is detached, the IP can be reduced significantly to 98.6 kcal/mol. This indicates that the proton separation is helpful for oxidation. The binding of **HIDAIH** with a water molecule through the N—H…O bond is an exothermic reaction; 7.0 kcal/mol energy is released. For the oxidized **HIDAIH**$^+$ system the hydration process is more exothermic. The binding energy of **HIDAIH**$^+$ with water is 14.2 kcal/mol. Unlike proton detachment from water, it is more convenient to detach one electron from the system. The corresponding IP is 89.2 kcal/mol, about half of that of **HIDAIH**.

Thus, the basic environment is in favor of the ionization, while the effect of the neutral condition is indistinctive. To prevent the DNA mutation, it is better to provide the weak acidic environment.

CONCLUSIONS

The trustworthy B3LYP/6-311+G***** method is employed to investigate the imidazole-dehydrogenated adenine-imidazole system in terms of the geometric structure, IR spectroscopy, electron population, and the adiabatic ionization potential.

Proton transfer occurs spontaneously upon oxidation from the amido group to the adjacent imidazole fragment. The larger the pH value of the environment, the significant the influence on the geometric structure is. The electron population on the HOMO determines the IR vibrational frequency of the H bond being blue-shifted or red-shifted upon oxidation. The complex prefers to be oxidized under the basic condition. The weak acidic environment is recommended to prevent the DNA mutation.

REFERENCES

1. *Best G.C., Dervan P.B.* // J. Amer. Chem. Soc. – 1995. – **117**. – P. 1184.
2. *Pundlik S.S., Gadre S.R.* // J. Phys. Chem. B. – 1997. – **101**. – P. 9657.
3. *Shields G.C., Laughton C.A., Orozco M.* // J. Amer. Chem. Soc. – 1997. – **119**. – P. 7463.
4. *Robles J., Grandas A., Pedroso E., Luque F.J., Eritja R., Orozco M.* // Curr. Org. Chem. – 2002. – **6**. – P. 1333.
5. *Peters M., Rozas I., Alkorta I., Elguero J.* // J. Phys. Chem. B. – 2003. – **107**. – P. 323.
6. *Daycock J.T., Jones G.P., Evans J.R.N., Thomas J.M.* // Nature. – 1968. – **218**. – P. 672.
7. *Kawada A., McGhie A.R., Labes M.M.* // J. Chem. Phys. – 1970. – **52**. – P. 3121.
8. *Colombo L., Bleckmann P., Schrader B., Schneider R., Plesser Th.* // J. Chem. Phys. – 1974. – **61**. – P. 3270.
9. *Loeffen P.W., Pettifer R.F., Fillaux F., Kearley G.J.* // J. Chem. Phys. – 1995. – **103**. – P. 8444.
10. *Hickman B.S., Mascal M., Titman J.J., Wood I.G.* // J. Amer. Chem. Soc. – 1999. – **121**. – P. 11486.

11. *Su C.C., Chang H.C., Jiang J.C., Wei P.Y., Lu L.C., Lin S.H.* // J. Chem. Phys. – 2003. – **119**. – P. 10753.
12. *Basch H., Krauss M., Stevens W.J.* // J. Amer. Chem. Soc. – 1985. – **107**. – P. 7267.
13. *Scheiner S., Yi M.Y.* // J. Phys. Chem. – 1996. – **100**. – P. 9235.
14. *Münch W., Kreuer K.D., Silvestri W., Maier J., Seifert G.* // Solid State Ionics. – 2001. – **145**. – P. 437.
15. *Yan S., Bu Y., Cao Z., Li P.* // J. Phys. Chem. A. – 2004. – **108**. – P. 7038.
16. *Russo N., Toscano M., Grand A., Jolibois F.* // J. Comp. Chem. – 1998. – **19**. – P. 989.
17. *Conti I., Garavelli M., Orlandi G.* // J. Amer. Chem. Soc. – 2009. – **131**. – P. 16108.
18. *Verma S., Mishra A.K., Kumar J.* // Acc. Chem. Res. – 2010. – **43**. – P. 79.
19. *Acocella A., Jones G.A., Zerbetto F.* // J. Phys. Chem. B. – 2010. – **114**. – P. 4101.
20. *Gohlke S., Abdoul-Carime H., Illenberger E.* // Chem. Phys. Lett. – 2003. – **380**. – P. 595.
21. *Li X., Sevilla M.D., Sanche L.* // J. Phys. Chem. B. – 2004. – **108**. – P. 19013.
22. *Bera P.P., Schaefer H.F.* // Proc. Natl. Acad. Sci. U.S.A. – 2005. – **102**. – P. 6698.
23. *Lind M.C., Bera P.P., Richardson N.A., Wheeler S.E., Schaefer H.F.* // Proc. Natl. Acad. Sci. U.S.A. – 2006. – **103**. – P. 7554.
24. *Xie H., Xia F., Cao Z.* // J. Phys. Chem. A. – 2007. – **111**. – P. 4384.
25. *Churchill C.D.M., Wetmore S.D.* // J. Phys. Chem. B. – 2009. – **113**. – P. 16046.
26. *Cui P.Y., Meng L.Q., Liu B.P.* // Struct. Chem. – 2010. – **21**. – P. 873.
27. *Nir E., Janzen C., Imhof P., Kleinermanns K., de Vries M.S.* // Phys. Chem. Chem. Phys. – 2002. – **4**. – P. 740.
28. *Plützer C., Hünig I., Kleinermanns K.* // Phys. Chem. Chem. Pys. – 2003. – **5**. – P. 1158.
29. *Yan S., Zhang L., Cukier R.I., Bu Y.* // Chem. Phys. Chem. – 2007. – **8**. – P. 944.
30. *Frisch M.J., Trucks G.W., Schlegel H.B., Scuseria G.E., Robb M.A., Cheeseman J.R., Montgomery J.A. Jr., Vreven T., Kudin K.N., Burant J.C., Millam J.M., Iyengar S.S., Tomasi J., Barone V., Mennucci B., Cossi M., Scalmani G., Rega N., Petersson G.A., Nakatsuji H., Hada M., Ehara M., Toyota K., Fukuda R., Hasegawa J., Ishida M., Nakajima T., Honda Y., Kitao O., Nakai H., Klene M., Li X., Knox J.E., Hratchian H.P., Cross J.B., Bakken V., Adamo C., Jaramillo J., Gomperts R., Stratmann R.E., Yazyev O., Austin A.J., Cammi R., Pomelli C., Ochterski J.W., Ayala P.Y., Morokuma K., Voth G.A., Salvador P., Dannenberg J.J., Zakrzewski V.G., Dapprich S., Daniels A.D., Strain M.C., Farkas O., Malick D.K., Rabuck A.D., Raghavachari K., Foresman J.B., Ortiz J.V., Cui Q., Baboul A.G., Clifford S., Cioslowski J., Stefanov B.B., Liu G., Liashenko A., Piskorz P., Komaromi I., Martin R.L., Fox D.J., Keith T., Al-Laham M.A., Peng C.Y., Nanayakkara A., Challacombe M., Gill P.M.W., Johnson B., Chen W., Wong M.W., Gonzalez C., Pople J.A.* Gaussian 03, Gaussian, Inc., Wallingford CT, 2004.
31. *Russo N., Toscano M., Grand A.* // J. Comput. Chem. – 2000. – **21**. – P. 1243.
32. *Wieczorek R., Dannenberg J.J.* // J. Amer. Chem. Soc. – 2003. – **125**. – P. 14065.
33. *Hobza P., Havlas Z.* // Chem. Rev. – 2000. – **100**. – P. 4253.
34. *Joseph J., Jemmis E.D.* // J. Amer. Chem. Soc. – 2007. – **129**. – P. 4620.